

Bull. Pure Appl. Sci. Sect. E Math. Stat. **39E**(1), 122–136 (2020) e-ISSN:2320-3226, Print ISSN:0970-6577 DOI: 10.5958/2320-3226.2020.00012.0 ©Dr. A.K. Sharma, BPAS PUBLICATIONS, 387-RPS- DDA Flat, Mansarover Park, Shahdara, Delhi-110032, India. 2020

Bulletin of Pure and Applied Sciences Section - E - Mathematics & Statistics

Website: https://www.bpasjournals.com/

# Flow characteristics of unsteady MHD Newtonian fluid past a rotating vertical porous plate \*

P. Chandra Reddy<sup>1,†</sup>, N. Veera Mohan Reddy<sup>2</sup> and C. Srinivasulu<sup>3</sup>

1,2,3. Department of Mathematics, Annamacharya Institute of Technology and Sciences (Autonomous), Rajampet, Andhra Pradesh-516126, India.

1. E-mail: chandramsc01@gmail.com

Abstract A theoretical analysis with numerical solutions is performed to explain the flow characteristics of an unsteady MHD Newtonian fluid along a vertical porous plate with rotation under the existence of heat and mass transfer. The governing equations of the flow pattern are converted to non-dimensional form and then solved by using finite difference scheme. The effects of different physical parameters like thermal radiation, heat source and sink, thermal diffusion and Dufour number are considered. The impact of these parameters on the fluid velocity, temperature and species concentration is depicted in the form of numerical results and graphical presentations. The current results are compared with the previously published ones and they confirm the correctness of the numerical method. The primary velocity of the fluid increases when the value of rotation parameter increases and the secondary velocity decreases in the same case.

**Key words** Rotating fluid, Thermal radiation, finite difference scheme, Soret number and Dufour effect.

**2020** Mathematics Subject Classification 76M20, 76S05, 76S99, 76U05, 76U99, 76W05, 76W99.

#### 1 Introduction

Rotating flows through porous media have received extensive importance in the modern research in computational fluid dynamics. Tremendous treatises on this area with applications in geophysics and planetary sciences have been in existence in the literature since the early 1950's. The joint impacts of heat and mass transfer in rotational hydrodynamics have largely been inspired due to their applications in chemical engineering and manufacturing processes in the industries.

The theoretical concepts of rotating fluids are given by Greenspan [1]. Hydrodynamic resistance and the heat loss of rotating solids are established by Dorfman [2]. Kreith [3] invented the convective mode of heat transfer in rotating fields. The detailed information on higher order heat transfer from a rotating sphere was given by Takhar and Whitelaw [4]. Hossain and Takhar [5] considered the rotating bodies and established radiation-conduction interaction in mixed convection. Naroua et al. [6] explained natural convection flow of rotating fluids with finite element method under the existence of radiation mode of heat transfer. The nature of the fluid flow along an accelerated horizontal plate in

<sup>\*</sup> Communicated, edited and typeset in Latex by *Lalit Mohan Upadhyaya* (Editor-in-Chief). Received February 26, 2019 / Revised December 17, 2019 / Accepted January 13, 2020. Online First Published on June 30, 2020 at https://www.bpasjournals.com/.

<sup>&</sup>lt;sup>†</sup>Corresponding author P. Chandra Reddy, E-mail: chandramsc01@gmail.com

a rotating fluid was given by Deka et al. [7]. Debnath [8] established exact solutions of the unsteady hydrodynamic and hydromagnetic boundary layer equations in a rotating fluid system. Sarojamma and Krishna [9] considered and analyzed transient hydromagnetic convective flow in rotating channel with porous boundaries. Smirnov and Shatrov [10] analyzed the development of the boundary layer on a plate in a rotating system. Page [11] reported the low Rossby number flow of a rotating fluid past a flat plate. Wang [12] found the process of stretching a surface in a rotating fluid. Takhar and Nath [13] established unsteady flow over a stretching surface in a rotating fluid under the presence of magnetic field. Ganapathy [14] reviewed and gave a note on oscillatory Couette flow in a rotating system. Singh [15] and Singh et al. [16] found an oscillatory hydromagnetic Couette flow in a rotating system and also evaluated a periodic solution of oscillatory Coutte flow through porous medium in rotating system. Ghosh [17] established the nature of unsteady hydromagnetic flow in a rotating channel with oscillating pressure gradient. Seth et al. [18, 19, 20] explained hydromagnetic oscillatory Couette flow in a rotating system by taking various parameters. MHD transient flow past an impulsively started horizontal porous plate in a rotating system with Hall current was discussed by Ahmed and Sarmah [21]. In order to examine the flow pattern under the influence of Soret and Dufour effects we have gone through the articles which involves these effects. Tsai and Huang [22] considered heat and mass transfer for Soret and Dufour's effects on Hiemenz flow through porous medium onto a stretching surface. Narayana and Murthy [23] established Soret and Dufour effects in a doubly stratified Darcy porous medium. Narayana and Sibanda [24] analyzed Soret and Dufour effects on free convection along a vertical wavy surface in a fluid saturated Darcy porous medium. Alam et al. [25] illustrated cross diffusion effects on steady free convection and mass transfer flow through porous medium. Makinde and Olanrewaju [26] considered these effects under mixed convection through a binary mixture of chemically reacting fluid. Mishra et al. [27] discussed in detail the chemical reaction and Soret effects on hydromagnetic micropolar fluid along a stretching sheet. Rashidi et al. [28] evaluated and explained group theory and differential transform analysis of mixed convective heat and mass transfer from a horizontal surface with chemical reaction effects. Kumar and Singh [29] established the impact of induced magnetic field on unforced convection in vertical concentric annuli under the existence of Newtonian heating/cooling. Mythili and Sivaraj [30] found the impact levels of higher order chemical reaction and non-uniform heat source/sink on Casson fluid flow over a vertical cone and flat plate. Sandeep et al. [31] selected 3D-Casson fluid flow embedded by a surface at absolute zero under modified viscosity model. Abbasi and Shehzad [32] gave conclusions for heat transfer analysis for three-dimensional flow of Maxwell fluid with thermal conductivity by applying the Cattaneo-Christov heat flux model. Deka et al. [33] analyzed transient free convection MHD flow past a vertical plate immersed in porous medium with exponentially decaying wall temperature and radiation.

In view of the findings from the above studies we consider here the flow of an unsteady MHD heat and mass transfer Newtonian fluid past a vertical porous plate with rotation and its properties are pointed out. This study is the extension of the article by Deka et al. [33] with the novelty of including rotation parameter, heat generation, chemical reaction and cross-diffusion effects.

#### 2 Mathematical formulation

The laminar flow of a rotating fluid past a porous plate in conducting field with variable temperature and variable concentration taking into account the chemical reaction, radiation, thermal diffusion and Dufour effects is considered. X-axis is taken along the plate which is in vertical direction. Y-axis is taken normal to the surface of the plate. The plate as well as the fluid in a state of rigid body rotates with a uniform angular velocity  $\Omega$  about Y-axis. Initially at time  $t^* \leq 0$ , both the fluid and the plate are at rest with uniform temperature and concentration  $T_{\infty}$  and  $C_{\infty}$  respectively. At time  $t^* > 0$ , the plate starts moving in the X direction with uniform velocity  $U_0 a^* t^*$ . The temperature and concentration rises to  $T_{\infty} + (T_s^* - T_{\infty}) \left(\frac{t^*}{t_0}\right)$  and  $C_{\infty} + (C_s^* - C_{\infty}) \left(\frac{t^*}{t_0}\right)$  respectively. Later it is maintained at uniform temperature and concentration  $T_{\infty}$  and  $C_{\infty}$  respectively. Under these considerations the equations that govern the flow are as follows:

$$\frac{\partial u^*}{\partial t^*} + 2\Omega V^* = \nu \frac{\partial^2 u^*}{\partial y^{*2}} + g\beta_T (T^* - T_\infty) + g\beta_C (C^* - C_\infty) - \frac{\sigma B_0^2 u^*}{\rho} - \frac{\nu}{k} u^*$$
 (2.1)



$$\frac{\partial V^*}{\partial t^*} - 2\Omega u^* = \nu \frac{\partial^2 V^*}{\partial u^{*2}} - \frac{\sigma B_0^2 V^*}{\rho} - \frac{\nu}{k} V^*$$
(2.2)

$$\rho C_p \frac{\partial T^*}{\partial t^*} = k_T \frac{\partial^2 T^*}{\partial y^{*2}} + Q^* \left( T^* - T_\infty \right) - \frac{\partial q_r^*}{\partial y^*} + \frac{D_m k_T \rho}{C_s} \frac{\partial^2 C^*}{\partial y^{*2}}$$

$$(2.3)$$

$$\frac{\partial C^*}{\partial t^*} = D \frac{\partial^2 C^*}{\partial y^{*2}} - K_r^* (C^* - C_\infty) + D_1 \frac{\partial^2 T^*}{\partial y^{*2}}$$

$$\tag{2.4}$$

The corresponding initial and boundary conditions are

$$u^{*} = 0, \ V^{*} = 0, T^{*} = T_{\infty}, \ C^{*} = C_{\infty} \text{ for all } y^{*}, t^{*} \leq 0$$

$$t^{*} > 0: \ u^{*} = U_{0}a^{*}t^{*}, V^{*} = U_{0}a^{*}t^{*}, T^{*} = T_{\infty} + (T_{s}^{*} - T_{\infty})\left(\frac{t^{*}}{t_{0}}\right),$$

$$C^{*} = C_{\infty} + (C_{s}^{*} - C_{\infty})\left(\frac{t^{*}}{t_{0}}\right) \text{ at } y^{*} = 0,$$

$$u^{*} = 0, \ T^{*} = T_{\infty}, \ C^{*} = C_{\infty} \text{ as } y^{*} \to \infty$$

$$(2.5)$$

The term  $\frac{\partial q_r^*}{\partial y^*}$  in equation (2.3) represents the change in the radiative flux with the distance normal to the plate. For an optically thin gray gas, the local radiant is given by the relation

$$\frac{\partial q_r^*}{\partial y^*} = 4a'\sigma^* \left(T_{\infty}^{*^4} - T^{*^4}\right)$$

where  $\sigma^*$  and a' are the Stefan-Boltzmann constant and mean absorption co-efficient respectively. We assume that the differences within the flow are sufficiently small so that  $T^{*4}$  can be expressed as a linear function of  $T^*$  after using Taylor's series to expand  $T^{*4}$  about the free stream temperature  $T_{\infty}^{*4}$  and neglecting higher order terms. This results in the following approximation:  $T^{*4} \cong 4T_{\infty}^{*3}T^* - 3T_{\infty}^{*4}$ . Then equation (2.2) takes the following form

$$\rho C_p \frac{\partial T^*}{\partial t^*} = k \frac{\partial^2 T^*}{\partial u^{*2}} + q_0 \left( T^* - T_{\infty}^* \right) - 16a' \sigma^* T_{\infty}^{*3} \left( T^* - T_{\infty}^* \right)$$
 (2.6)

The non-dimensional quantities are as follows:

$$u = \frac{u^*}{U_0}, \ V = \frac{V^*}{U_0}, t = \frac{t^*U_0^2}{\nu}, \ y = \frac{y^*U_0}{\nu}, \ \theta = \frac{T^* - T_\infty}{T_s^* - T_\infty}, \ C = \frac{C^* - C_\infty}{C_s^* - C_\infty}, \ a = \frac{a^*\nu}{U_0^2}, \ \frac{\partial q_r^*}{\partial y^*} = 4(T^* - T_\infty)I^*,$$

$$Gr = \frac{\nu g \beta_T \left(T_s^* - T_\infty\right)}{U_0^3}$$
, (Grashof number)

$$Gr = \frac{\nu g \beta_T \left(T_s^* - T_\infty\right)}{U_0^3}, \text{ (Grashof number)}$$

$$Gm = \frac{\nu g \beta_C \left(C_s^* - C_\infty\right)}{U_0^3}, \text{ (Modified Grashof number)}$$

$$M = \frac{\sigma B_0^2 \nu}{\rho U_0^2}$$
, (Magnetic parameter)  
 $k_1^2 = \frac{\Omega \nu}{U_0^2}$ , (Rotation parameter)

$$k_1^2 = \frac{\Omega \nu}{U^2}$$
, (Rotation parameter)

$$K = \frac{kU_0^2}{\nu^2}, \text{(Permeability of the porous medium)}$$

$$\text{Pr} = \frac{\rho\nu C_p}{k_T}, \text{(Prandtl number)}$$

$$Q = \frac{Q^*\nu^2}{k_T U_0^2}, \text{ (Heat absorption)}$$

$$F = \frac{4\nu I^*}{\rho C_p U_0^2}, \text{(Radiation parameter)}$$

$$Sc = \frac{\nu}{\nu} \text{ (Schmidt number)}$$

$$Pr = \frac{\rho \nu C_p}{k_T}$$
, (Prandtl number)

$$Q = \frac{Q^* \nu^2}{k_T U_0^2}$$
, (Heat absorption)

$$F = \frac{4\nu I^*}{\rho C_p U_0^2}$$
, (Radiation parameter)

$$Sc = \frac{\nu}{D}$$
, (Schmidt number)

$$S_0 = \frac{D_1(T_s^* - T_\infty)}{\nu(C^* - C_\infty)}$$
 (Soret number)

$$Df = \frac{D_m k_T (C_s^* - C_\infty)}{\nu C_s C_p (T_s^* - T_\infty)}$$
 (Dufour number)

$$Sc = \frac{\nu}{D}, \text{ (Schmidt number)}$$

$$Sc = \frac{\nu}{D}, \text{ (Schmidt number)}$$

$$S_0 = \frac{D_1(T_s^* - T_\infty)}{\nu(C_s^* - C_\infty)} \text{ (Soret number)}$$

$$Df = \frac{D_m k_T(C_s^* - C_\infty)}{\nu C_s C_P(T_s^* - T_\infty)} \text{ (Dufour number)}$$

$$Kr = \frac{K_s^* \nu^2}{U_0^2}, \text{ (Chemical reaction parameter)}$$
Introducing the non-dimensional quantities

Introducing the non-dimensional quantities, the equations (2.1)–(2.4) reduces to following form

$$\frac{\partial u}{\partial t} + 2k_1^2 V = \frac{\partial^2 u}{\partial y^2} + Gr \theta + Gm C - M u - \frac{1}{K} u$$
 (2.7)



$$\frac{\partial V}{\partial t} - 2k_1^2 u = \frac{\partial^2 V}{\partial u^2} - MV - \frac{1}{K}V \tag{2.8}$$

$$\frac{\partial \theta}{\partial t} = \frac{1}{\Pr} \frac{\partial^2 \theta}{\partial y^2} + Q\theta - F\theta + Df \frac{\partial^2 C}{\partial y^2}$$
 (2.9)

$$\frac{\partial C}{\partial t} = \frac{1}{Sc} \frac{\partial^2 C}{\partial u^2} - KrC + S_0 \frac{\partial^2 \theta}{\partial u^2}$$
 (2.10)

The corresponding initial and boundary conditions are

$$\begin{array}{l} u = 0, \ V = 0, \ \theta = 0, \ C = 0 & \text{for all} \ y, t \le 0 \\ t > 0: \ u = e^{at}, V = e^{at}, \ \theta = t, \ C = t \ \text{at} \ y = 0 \\ u = 0, \ V = 0, \ \theta = 0, \ C = 0 & \text{as} \ y \to \infty \end{array}$$

#### 3 Method of solution

We observe that (2.7)–(2.10) are linear partial differential equations and they are to be solved with the initial and boundary conditions (2.11). In fact the exact solution is not possible for this set of equations and hence we solve these equations by finite-difference method.

The equivalent finite difference schemes of equations for (2.7)–(2.10) are as follows:

$$\frac{u_{i,j+1} - u_{i,j}}{\Delta t} + 2k_1^2 V_{i,j} = Gr \,\theta_{i,j} + Gm \,C_{i,j} + \frac{u_{i-1,j} - 2 \,u_{i,j} + u_{i+1,j}}{(\Delta y)^2} - M \,u_{i,j} - \frac{1}{K} \,u_{i,j} \tag{3.1}$$

$$\frac{V_{i,j+1} - V_{i,j}}{\Delta t} - 2k_1^2 u_{i,j} = \frac{V_{i-1,j} - 2V_{i,j} + V_{i+1,j}}{(\Delta y)^2} - MV_{i,j} - \frac{1}{K}V_{i,j}$$
(3.2)

$$\frac{\theta_{i,j+1} - \theta_{i,j}}{\Delta t} = \frac{1}{\Pr} \frac{\theta_{i-1,j} - 2\theta_{i,j} + \theta_{i+1,j}}{(\Delta y)^2} + Q\theta_{i,j} - F\theta_{i,j} + Df \frac{C_{i-1,j} - 2C_{i,j} + C_{i+1,j}}{(\Delta y)^2}$$
(3.3)

$$\frac{C_{i,j+1} - C_{i,j}}{\Delta t} = \frac{1}{Sc} \frac{C_{i-1,j} - 2C_{i,j} + C_{i+1,j}}{(\Delta y)^2} - KrC_{i,j} + S_0 \frac{\theta_{i-1,j} - 2\theta_{i,j} + \theta_{i+1,j}}{(\Delta y)^2}$$
(3.4)

Here, the suffixes "i" refer to "y" and "j" to time. The mesh system is divided by taking  $\Delta y = 0.1$ . From the initial condition in (2.11), we have the following equivalent:

$$u(i,0) = 0, \ V = 0, \ \theta(i,0) = 0, \ C(i,0) = 0 \ \forall i$$
 (3.5)

The boundary conditions from (2.11) are expressed in finite-difference form as follows

$$u(0,j) = e^{at}, \ V(0,j) = e^{at}, \ \theta(0,j) = t, \ C(0,j) = t \ \forall j$$
  

$$u(i_{\text{max}},j) = 0, \ u(i_{\text{max}},j) = 0, \ \theta(i_{\text{max}},j) = 0, \ C(i_{\text{max}},j) = 0 \ \ \forall j$$
(3.6)

(Here  $i_{max}$  is taken as 200.)

The primary velocity at the end of time step viz,  $u(i, j+1), i=1,\ldots,200$  is computed from (3.1) and the secondary velocity at the end of time step viz,  $V(i, j+1), i=1,\ldots,200$  is computed from (3.2) in terms of velocity, temperature and concentration at points on the earlier time-step. After that  $\theta(i, j+1)$  is computed from (3.3) and then C(i, j+1) is computed from (3.4). The procedure is repeated until t-0.5 (i.e., j=500). During computation  $\Delta t$  is chosen as 0.001.

# Skin-friction:

The skin-friction in non-dimensional form is given by the relation  $\tau = \left(\frac{du}{dy}\right)_{y=0}$ .

#### Rate of heat transfer:

The dimensionless rate of heat transfer in terms of Nusselt number is given by  $Nu = -\left(\frac{d\theta}{dy}\right)_{y=0}$ .

#### Rate of mass transfer:

The dimensionless rate of mass transfer in terms of Sherwood number is given by  $Sh = -\left(\frac{dC}{dy}\right)_{y=0}$ .



## 4 Results and discussion

The physical parameters involved in the flow are changed numerically and we observe their influence on velocity, temperature, concentration, local skin-friction coefficient, local Nusselt number (rate of heat transfer) and the local Sherwood number (rate of mass transfer). The graphical presentations and tables are helpful in this analysis. Initially the present methodology is verified by comparing a result with the previous literature of Deka et al. [33] in the absence of newly introduced parameters. It is evident from Fig. 1 that a good conformity is noticed among the present and previous results in the comparison. Figs. 2, 3 exhibit the velocity profiles with the effect of Grashof number for heat and mass transfer. It is noticed that the fluid velocity increases under the increment of both the cases of Grashof number and modified Grashof number. This is due to the presence of thermal and solutal buoyancy which has the tendency of leading to an increase in the velocity. The variation in velocity under diffusion thermo effect is depicted in Fig. 4. The velocity grows when the values of Dufour number increases. The effect of magnetic parameter on primary velocity and secondary velocity is illustrated in the Figs. 5, 6. The velocity falls down when the values of magnetic parameter increases. This is due to the application of transverse magnetic field, which has the tendency of reducing the velocity. This drag force is called the Lorentz force. The impact of porosity parameter on primary velocity and secondary velocity is presented in the Figs. 7, 8. The velocity grows for increasing values of porosity parameter. Figs. 9, 10 depict the changes in primary and secondary velocities under the influence of rotation parameter. The primary velocity falls down for enhancing values of rotation parameter but an opposite nature is observed in the case of secondary velocity. The variation in the primary velocity with the impact of thermal diffusion is shown in Fig. 11 and an improvement in the velocity is noticed. The consequence of Prandtl number on fluid temperature is shown in Fig. 12. It is evident that the temperature falls down when the value of Prandtl number is increased. The basic reason behind this nature is that the reduced fluid velocity would mean heat is not convected readily and hence the surface temperature decreases. The consequence in temperature in the existence of heat source and sink is exhibited in Fig. 13. It reveals that the temperature falls down under the influence of heat absorption parameter whereas the temperature grows in the presence of heat generation. The fact behind this effect is that the heat absorption causes a decrease in the kinetic energy as well as the thermal energy of the fluid. Hence the momentum and thermal boundary layers get thinner in case of heat absorbing fluids. Improved values of radiation parameter lead to a lessening in the temperature which is experienced from Fig. 14. Fig. 15 reveals that the temperature becomes thinner under the existence of thermal diffusion. The variations in temperature due to the impact of diffusion thermo effect are depicted in Fig. 16. The temperature grows for enhancing values of Dufour number. Fig. 17 illustrates the impact of Schmidt number on species concentration. It is noticed that as the Schmidt number increases, there is a decreasing trend in the concentration field. Not much of significant contribution of Schmidt number is observed far away from the plate. The variation in species concentration in the presence of chemical reaction is exhibited in Fig. 18. The existence of chemical reaction leads to a decrease the concentration of the fluid. Fig. 19 reveals that the concentration of the fluid enhances under the existence of thermal diffusion.

The variations in skin friction under the impact of the physical parameters are observed with the help of numerical values from Table 2. The primary skin friction as well as the secondary skin friction decreases for increased values of Grashof number and modified Grashof number but a reverse trend is seen in the case of magnetic field parameter and porosity parameter. The primary skin friction increases under the influence of rotation parameter and the secondary skin friction enhances when the values of rotation parameter are increased. Table 1 presents the effects of Prandtl number, heat source parameter, radiation parameter and Dufour number on skin friction and Nusselt number. The primary skin friction as well as the secondary skin friction decreases for increased values of radiation parameter but an opposite nature is found in the case of diffusion thermo effect. The rate of heat transfer rises on increasing the values of the Prandtl number, the radiation parameter and the Dufour number and on decreasing the values of the heat source parameter. Table 3 gives numerical illustration of the changes in Sherwood number. The Sherwood number increases under the influence of chemical reaction and Schmidt number whereas an opposite trend is noticed in the case of Soret number.



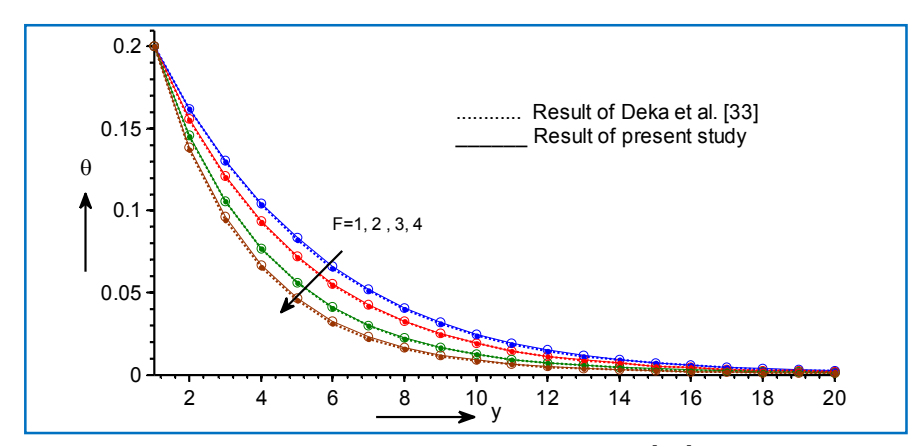


Fig. 1: Comparison of present result with that of Deka et al. [33] in the absence of porosity parameter, thermal diffusion, radiation, mass diffusion and rotation parameter.

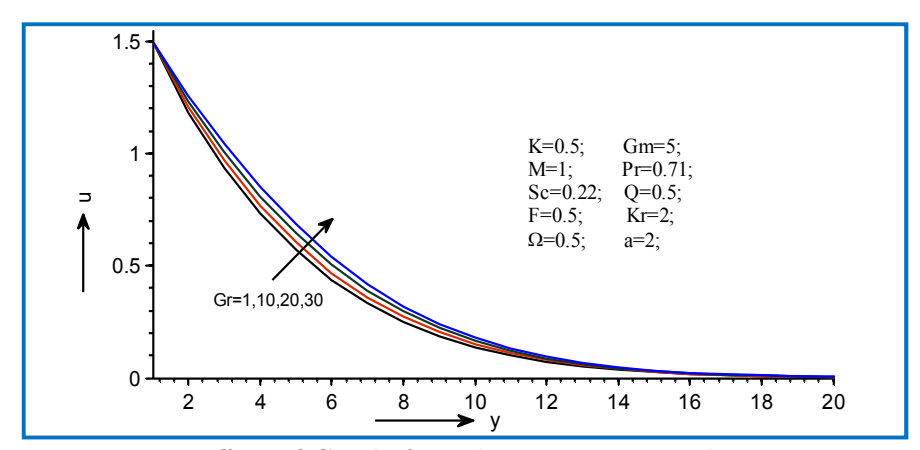


Fig. 2: Effect of Grashof number on primary velocity.

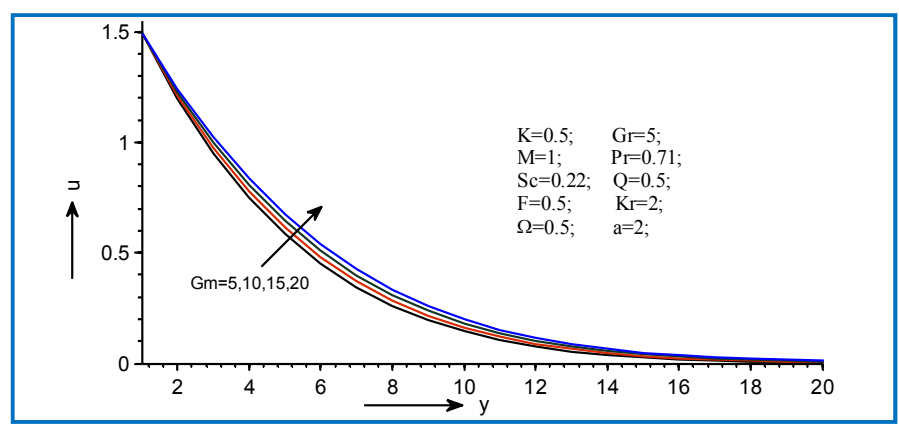


Fig. 3: Effect of modified Grashof number on primary velocity.



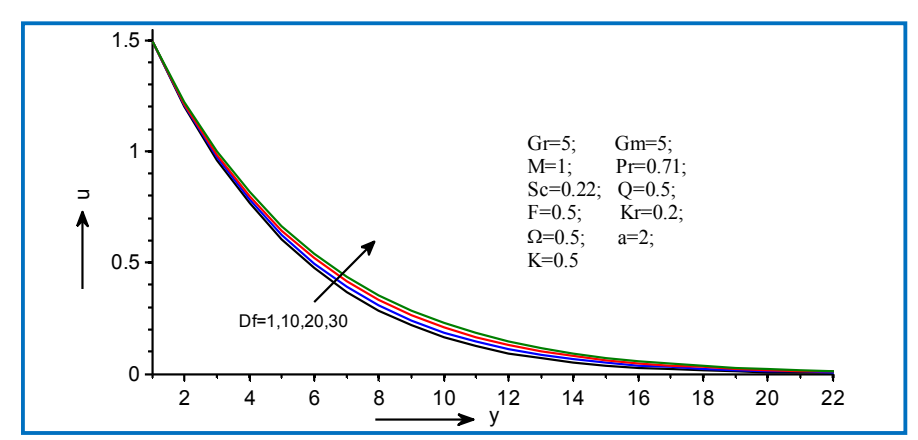


Fig. 4: Effect of Dufour number on primary velocity.

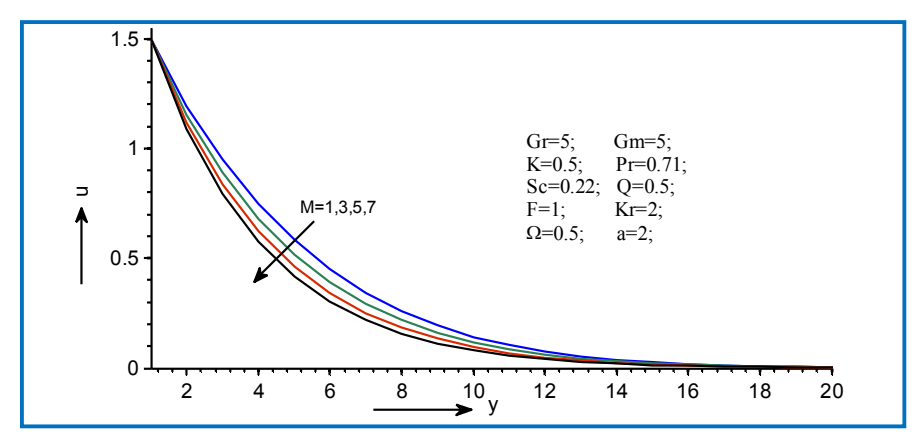


Fig. 5: Effect of magnetic parameter on primary velocity.

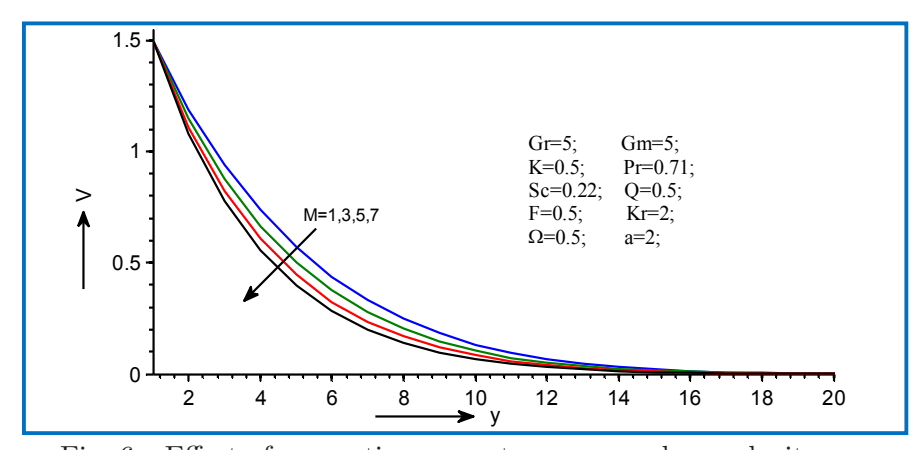


Fig. 6: Effect of magnetic parameter on secondary velocity.



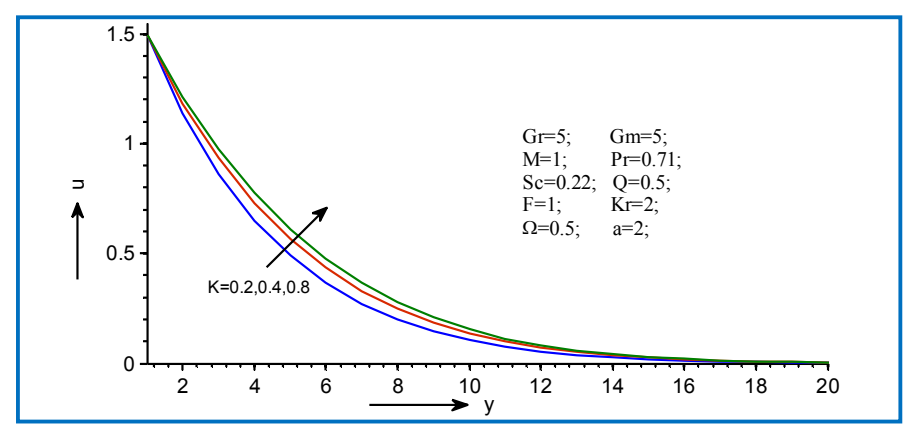


Fig. 7: Effect of porosity parameter on primary velocity.

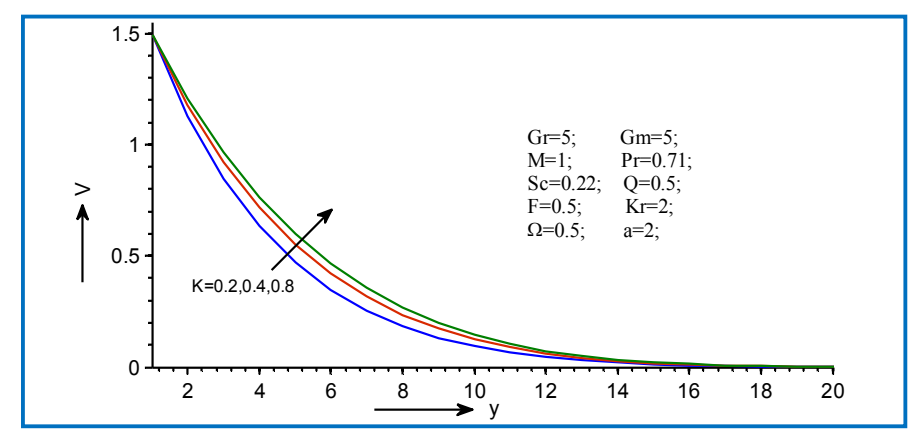


Fig. 8: Effect of porosity parameter on secondary velocity.

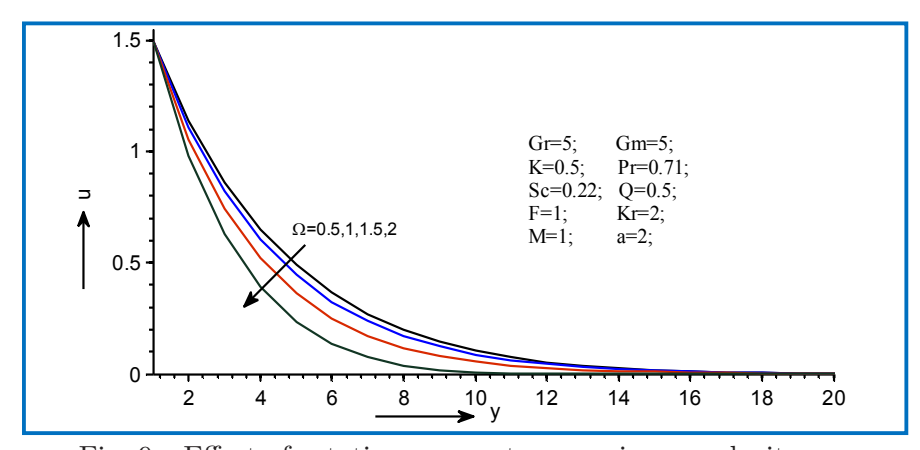


Fig. 9: Effect of rotation parameter on primary velocity.



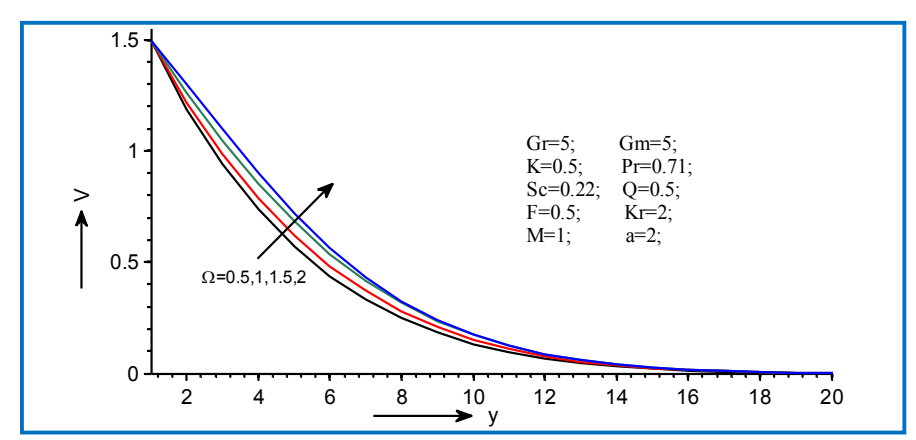


Fig. 10: Effect of rotation parameter on secondary velocity.

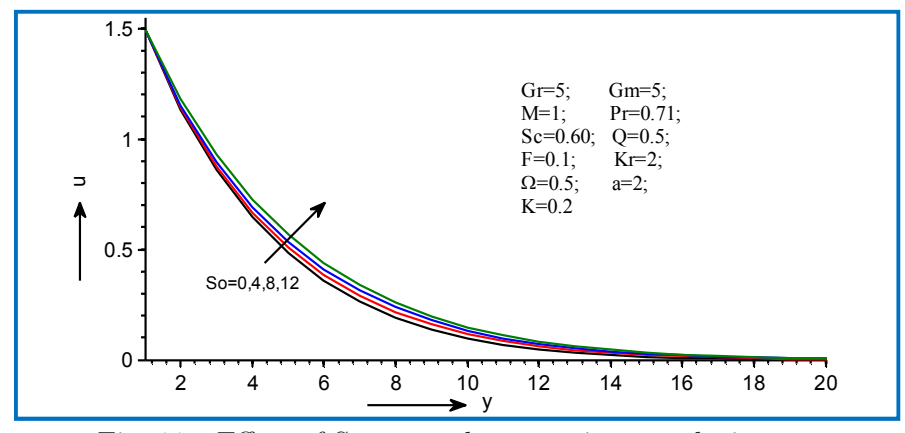


Fig. 11: Effect of Soret number on primary velocity.

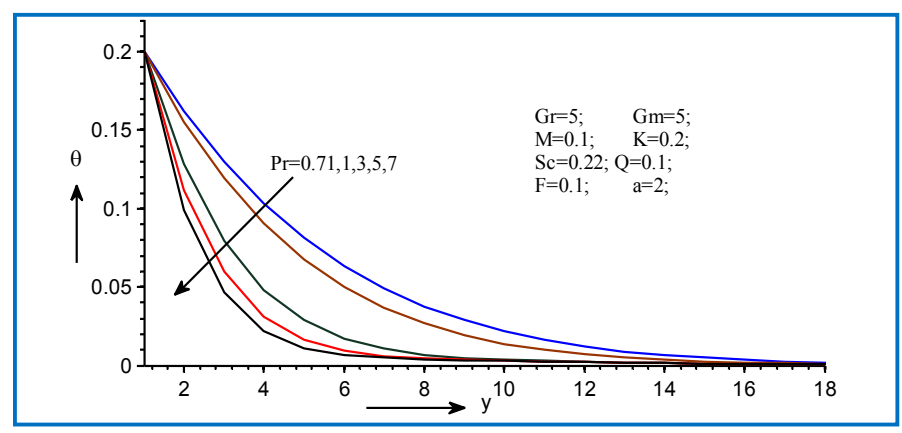


Fig. 12: Effect of Prandtl number on temperature.



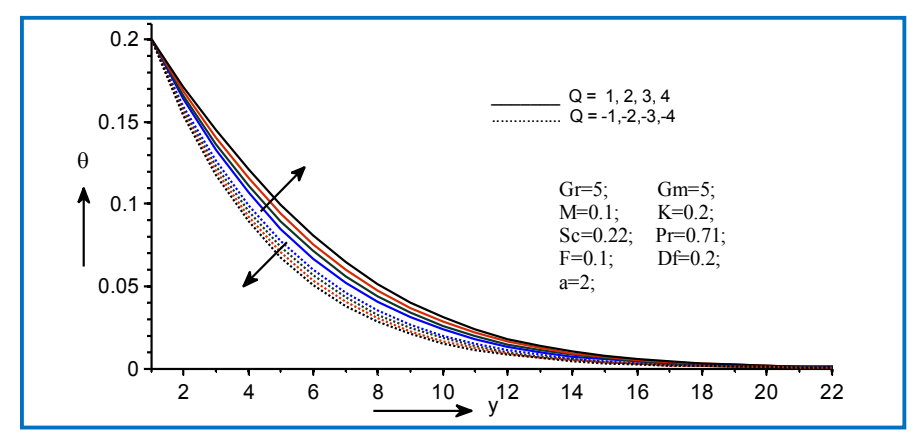


Fig. 13: Effect of heat source and sink parameters on temperature.

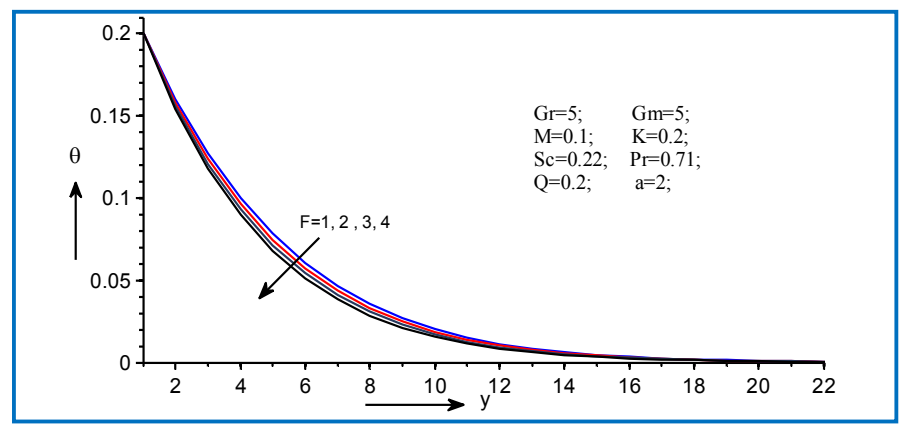


Fig. 14: Effect of radiation parameter on temperature.

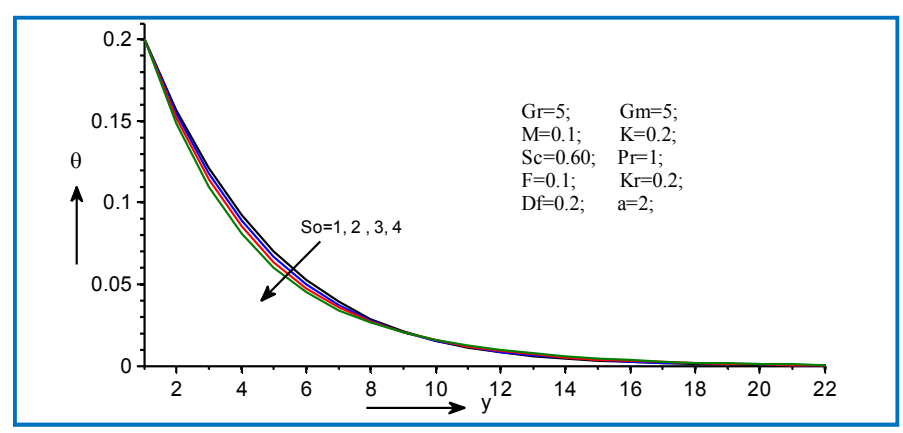


Fig. 15: Effect of Soret number on temperature.



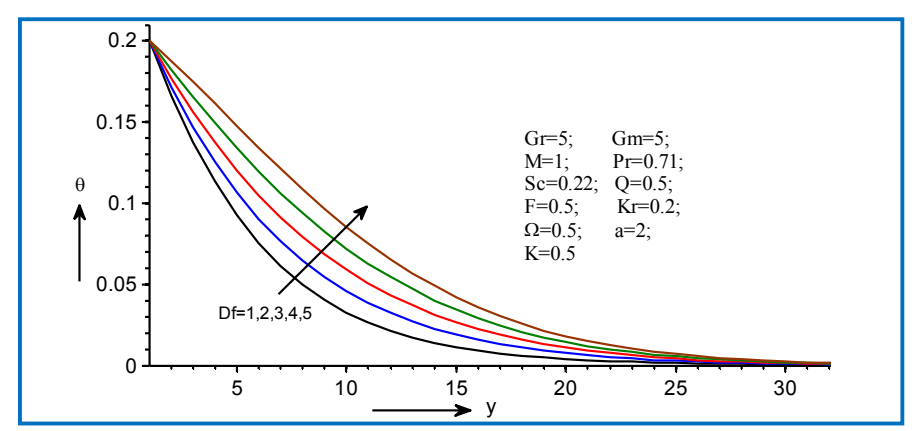


Fig. 16: Effect of Dufour number on temperature.

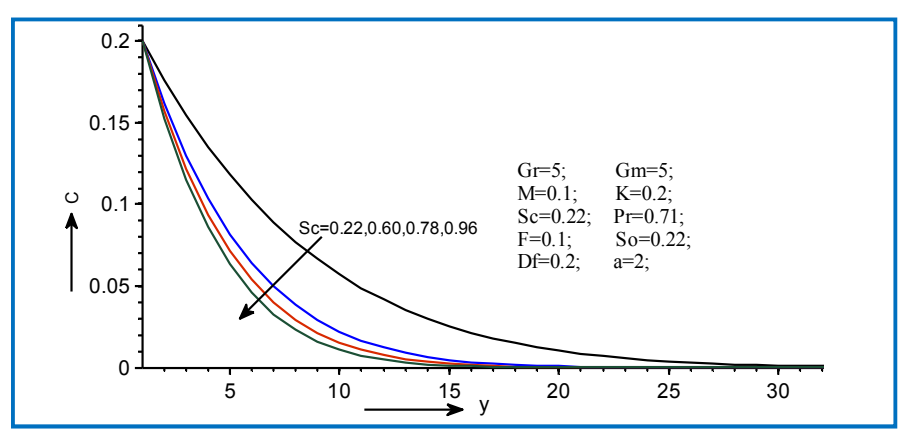


Fig. 17: Effect of Schmidt number on concentration.

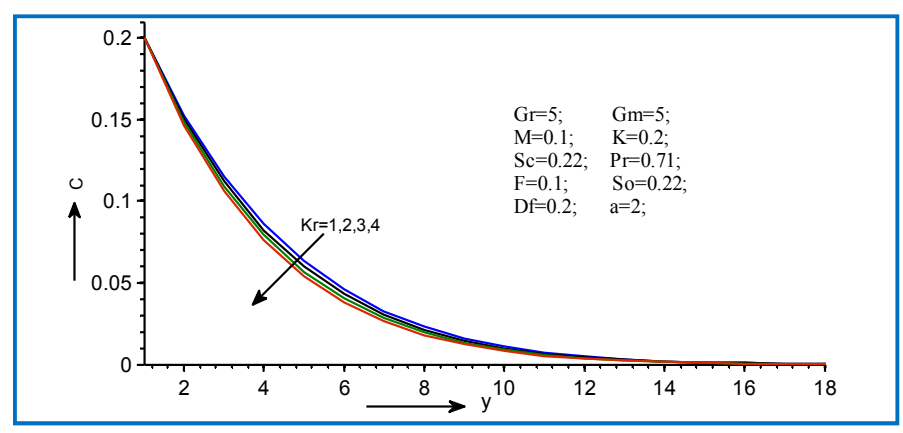


Fig. 18: Effect of chemical reaction parameter on concentration.



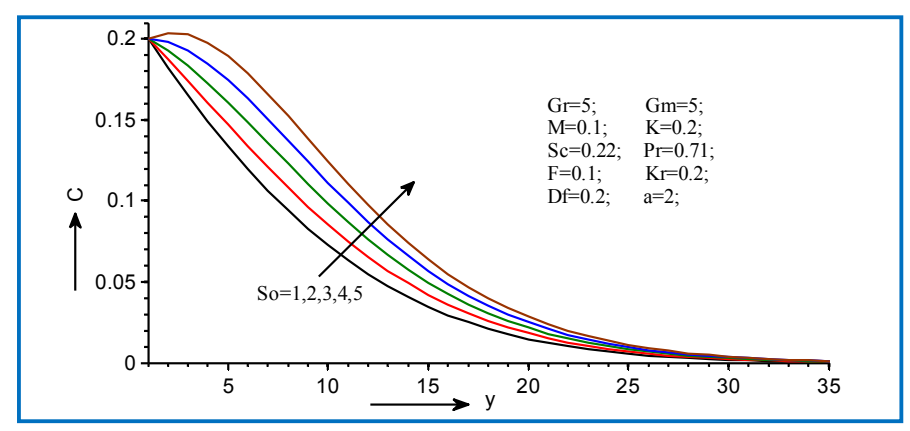


Fig. 19: Effect of Soret number on concentration.

Table 1: Variations in skin friction and Nusselt number under the influence of Prandtl number, heat source parameter and radiation parameter.

Pr	Q	F	Df	$ au_x$	$ au_y$	Nu
2	1	0.22	1	2.2134	0.0111	2.4191
4	1	0.22	1	1.5995	0.0288	4.4674
5	1	0.22	1	1.4054	0.0379	5.4853
2	1	0.22	1	1.2533	0.0471	2.5026
2	3	0.22	1	2.4729	0.0020	1.8595
2	4	0.22	1	2.3633	0.0031	1.0803
2	1	0.60	1	2.8319	0.1587	1.0492
2	1	0.78	1	2.7950	0.1488	1.0496
2	1	0.94	1	2.7366	0.1254	1.0498
2	1	0.22	1	2.9820	0.0847	1.1477
2	1	0.22	2	3.2820	0.1713	1.2472
2	1	0.22	3	3.7820	0.5178	1.6451



Table 2: Variations in skin friction under the influence of Grashof number modified Grashof number, magnetic parameter, porosity parameter and rotation parameter.

Gr	Gm	M	K	Ω	$ au_x$	$ au_y$
5	5	3	1.2	2.2	3.9445	0.0049
6	5	3	1.2	2.2	3.7070	0.0036
7	5	3	1.2	2.2	3.4695	0.0024
8	5	3	1.2	2.2	3.1321	0.0012
5	6	3	1.2	2.2	4.7479	0.2227
5	7	3	1.2	2.2	4.6309	0.1669
5	8	3	1.2	2.2	4.5138	0.0565
5	5	4	1.2	2.2	1.2790	0.0100
5	5	5	1.2	2.2	1.4619	0.0142
5	5	6	1.2	2.2	1.7387	0.0183
5	5	3	2.2	2.2	3.0392	0.0015
5	5	3	3.2	2.2	3.1400	0.0016
5	5	3	4.2	2.2	3.2403	0.0018
5	5	3	1.2	3.2	3.1162	0.0015
5	5	3	1.2	4.2	3.1264	0.0014
5	5	3	1.2	8.2	3.1369	0.0013

Table 3: Effect of chemical reaction parameter, Soret number and Schmidt number on skin friction and Sherwood number.

Kr	Sc	$S_0$	Sh
3	1	2	0.8081
5	1	2	1.2738
6	1	2	1.3198
3	1	2	0.1903
3	2	2	0.4004
3	3	2	0.9918
3	1	2	8.4572
3	1	4	7.9326
3	1	6	7.1524



## 5 Conclusions

The effects of different physical parameters like the thermal radiation, the heat source and sink, the chemical reaction, the thermal diffusion and the Dufour number are considered and the flow characteristics are examined. The summarized points of this study can be stated as follows:

- 1. The primary velocity of the fluid increases when the values of the rotation parameter increased and the secondary velocity decreases in the same case.
- 2. The temperature of the fluid enhances for increasing values of the heat source parameter and the Dufour number whereas a reverse trend is found in the case of the heat sink parameter, the Prandtl number, the radiation parameter and the Soret number.
- 3. The existence of thermal diffusion results in improving the concentration of the fluid whereas the chemical reaction leads to decrease it.
- 4. The primary skin friction increases under the influence of the rotation parameter and the secondary skin friction enhances when the values of rotation parameter are increased.
- 5. The rate of heat transfer rises for increasing values of the Prandtl number, the radiation parameter and the Dufour number and decreasing values of the heat source parameter.

#### References

- [1] Greenspan, H.P. (1968). The theory of rotating fluids, Cambridge University Press, New York.
- [2] Dorfman, L.A. (1963). Hydrodynamic resistance and the heat loss of rotating solids, Oliver & Boyd, Edinburgh.
- [3] Kreith, F. (1968). Convection heat transfer in rotating systems, in: Advances in Heat Transfer, Vol. 5, Academic Press, New York, 129–151.
- [4] Takhar, H.S. and Whitelaw, M.H. (1978). Higher order heat transfer from a rotating sphere, Acta Mechanica, 30, 101–109.
- [5] Hossain, M.A. and Takhar, H.S. (1997). Radiation-conduction interaction in mixed convection on rotating bodies, Heat Mass Transfer. Wärme-und Stoffübertragung, 33, 201–208.
- [6] Naroua, H., Ram, P.C., Sambo, A.S. and Takhar, H.S. (1998). Finite element analysis of natural convection flow in a rotative fluid with radiative heat transfer, *J. Magnetohydrodyn. Plasma Resch.*, 7, 257–274.
- [7] Deka, R.K., Gupta, A.S., Takhar, H.S. and Soundalgekar, V.M. (1999). Flow past an accelerated horizontal plate in a rotating fluid, *Acta Mechanica*, 30, 594–600.
- [8] Debnath, L. (1975). Exact solutions of the unsteady hydrodynamic and hydromagnetic boundary layer equations in a rotating fluid system, ZAMM, 55, 431–438.
- [9] Sarojamma, G. and Krishna, D.V. (1981). Transient hydromagnetic convective flow in rotating channel with porous boundaries, *Acta Mech.* 43, 49–54.
- [10] Smirnov, E.M. and Shatrov, A.V. (1982). Development of the boundary layer on a plate in a rotating system, Fluid Dyn., 17, 452–454.
- [11] Page, M.A. (1983). The low Rossby number flow of a rotating fluid past a flat plate, *J. Eng. Math.*, 17, 191–202.
- [12] Wang, C.Y. (1988). Stretching a surface in a rotating fluid, ZAMP, 39, 177–185.
- [13] Takhar, H.S. and Nath, G. (1998). Unsteady flow over a stretching surface with a magnetic field in a rotating fluid, ZAMP, 49, 989–1001.
- [14] Ganapathy, R. (1994). A note on oscillatory Couette flow in a rotating system,  $Trans.\ ASME\ J.\ Appl.\ Mech.,\ 61,\ 208–209.$
- [15] Singh, K.D. (2000). An oscillatory hydromagnetic Couette flow in a rotating system, ZAMM, 80, 429–432.
- [16] Singh, K.D., Gorla, M.G. and Hans, R. (2005). A periodic solution of oscillatory Couette flow through porous medium in rotating system, *Indian J. Pure Appl. Math.*, 36(3), 151–159.



- [17] Ghosh, S.K. (1993). Unsteady hydromagnetic flow in a rotating channel with oscillating pressure gradient, J. Phys. Soc. Jpn., 62, 3893–3903.
- [18] Seth, G.S., Nandkeolyar, R. and Ansari, S.Md. (2009). Hall effects on oscillatory hydromagnetic Couette flow in a rotating system, Int. J. Acad. Res., 1, 6-17.
- [19] Seth, G.S., Ansari, S.Md. and Nandkeolyar, R. (2011). Unsteady Hartmann flow in a rotating channel with perfectly conducting walls, Int. J. Appl. Mech. Eng., 16, 1129–1146.
- [20] Seth, G.S., Hussain, S.M. and Sarkar, S. (2014). Hydromagnetic oscillatory Couette flow in a rotating system with induced magnetic field, Appl. Math. Mech., 35, 1331–1344.
- [21] Ahmed, N. and Sarmah, H.K. (2011). MHD transient flow past an impulsively started horizontal porous plate in a rotating system with Hall current, *Int. J. Appl. Math and Mech.*, 7(2), 1–15.
- [22] Tsai, R. and Huang, J.S. (2009). Heat and mass transfer for Soret and Dufour's effects on Hiemenz flow through porous medium onto a stretching surface, *Int. J. Heat Mass Transf.*, 52, 2399–2406.
- [23] Narayana, P.L. and Murthy, P. (2007). Soret and Dufour effects in a doubly stratified Darcy porous medium, J. Porous Media, 10, 613–624.
- [24] Narayana, P.L. and Sibanda, P. (2010). Soret and Dufour effects on free convection along a vertical wavy surface in a fluid saturated Darcy porous medium, Int. J. Heat Mass Transfer, 53, 3030–3034.
- [25] Alam, M.S., Ferdows, M., Ota, M. and Maleque, M.A. (2006). Dufour and Soret effects on steady free convection and mass transfer flow past a semi-infinite vertical porous plate in a porous medium, Int. J. Appl. Mech. Eng., 11(3), 535–545.
- [26] Makinde, O.D. and Olanrewaju, P.O. (2011). Unsteady mixed convection with Soret and Dufour effects past a porous plate moving through a binary mixture of chemically reacting fluid, *Chem. Engg. Commun.*, 7, 920–938.
- [27] Mishra, S.R., Baag, S. and Mohapatra, D.K. (2016). Chemical reaction and Soret effects on hydromagnetic micropolar fluid along a stretching sheet, *Engineering Science and Technology*, 19(4), 1919–1928.
- [28] Rashidi, M.M., Rahimzadeh, N., Ferdows, M. and Jashim Uddin, Md. and Bég, O. Anwar (2012). Group theory and differential transform analysis of mixed convective heat and mass transfer from a horizontal surface with chemical reaction effects, Chemical Engineering Communications, 199(8), 1012–1043.
- [29] Kumar, D. and Singh, A.K. (2015). Effect of induced magnetic field on natural convection with Newtonian heating/cooling in vertical concentric annuli, *Procedia Eng.*, 127, 568–574.
- [30] Mythili, D. and Sivaraj, R. (2016). Influence of higher order chemical reaction and non-uniform heat source/sink on Casson fluid flow over a vertical cone and flat plate, J. Mol. Liq., 216, 466–475.
- [31] Sandeep, N., Koriko, O.K. and Animasaun, I.L. (2016). Modified kinematic viscosity model for 3D-Casson fluid flow within boundary layer formed on a surface at absolute zero, J. Mol. Liq., 221, 1197–1206.
- [32] Abbasi, F.M. and Shehzad, S.A. (2016). Heat transfer analysis for three-dimensional flow of Maxwell fluid with temperature dependent thermal conductivity: application of Cattaneo-Christov heat flux model, J. Mol. Liq., 220, 848–854.
- [33] Deka, R.K., Kalita, N. and Paul, A. (2015). Transient free convection MHD flow past a vertical plate immersed in porous medium with exponentially decaying wall temperature and radiation, Proceedings of International Conference on Frontiers in Mathematics (26-28 March, 2015 Department of Mathematics, Gauhati University Guwahati-781014 Assam, India. Conference Proceedings published in 2015 by Pratul Bhattacharyya, Shri Ganesh Printers, Noonmati, Guwahati. ISBN: 978-81-928118-9-5), 158-161.

